STATISTICS, OPTIMIZATION AND INFORMATION COMPUTING
Stat., Optim. Inf. Comput., Vol. **xx**, Month 2026, pp 0–22.
Published online in International Academic Press (www.IAPress.org)

Coordinated Active-Reactive BESS Scheduling via Convex Optimization with Degradation Costs

Oscar Danilo Montoya [1*], Fiderman Machuca-Martínez [2], Luis Fernando Grisales-Noreña [3]

[1] *Facultad de Ingeniería, Universidad Distrital Francisco José de Caldas, Bogotá D.C. 110121, Colombia*
[2] *Escuela de Ingeniería Química, CENM, Facultad de Ingeniería, Universidad del Valle, Cali 760015, Colombia*
[3] *Grupo de Investigación en Alta Tensión-GRALTA, Facultad de Ingeniería, Universidad del Valle, Cali 760015, Colombia*

Abstract The growing penetration of renewable energy sources in distribution networks, together with the increasing deployment of battery energy storage systems (BESS), calls for advanced operational frameworks that can coordinate active and reactive power dispatch while accounting for battery degradation and economic constraints. This paper proposes a novel convex optimization framework for the optimal day-ahead scheduling of BESS in active distribution networks. The problem is formulated as a mixed-integer nonlinear programming (MINLP) model that simultaneously optimizes the coordinated active and reactive power dispatch of BESS units while enforcing the power balance equation at each time interval for an aggregated single-node representation of the distribution network. Unlike most existing approaches that treat active and reactive power independently, the proposed formulation exploits the inverter capabilities of modern BESS units, enabling them to provide both energy arbitrage and reactive power support services at the same time. A detailed battery degradation cost model is incorporated using an equivalent full-cycle counting approach based on the cumulative variation of the state-of-charge trajectory, capturing the economic impact of cycling on battery lifetime. The resulting MINLP is exactly reformulated as a mixed-integer second-order cone program (MISOCP) through the convex reformulation of the apparent power constraints and the linearization of the absolute value terms in the degradation cost, preserving convexity and enabling efficient solution using state-of-the-art optimization solvers. The framework is implemented using MATLAB CVX with the Gurobi solver and validated on a modified 33-bus radial distribution network incorporating three PV generation units and three BESS units, with detailed time-varying load profiles, solar irradiance profiles, and energy price data representing realistic Colombian distribution system conditions. The computational analysis is organized around seven distinct scenarios that progressively introduce distributed energy resources and reactive power control capabilities. Numerical results show that the proposed framework achieves a total daily cost reduction of up to 50.28% compared to the base case without distributed resources, with PV integration alone reducing costs by 29.70%, and enabling reactive power control from PV inverters providing an additional 19.40% cost reduction. Furthermore, while BESS units operating with active power-only services provide minimal economic benefits, enabling reactive power control from BESS units yields a 10.37% cost reduction, and the full integration of both PV and BESS with coordinated active-reactive control achieves the best performance with a 50.28% cost reduction. The results confirm that coordinated active-reactive power dispatch, combined with degradation-aware scheduling, provides significant economic benefits for distribution systems with integrated renewable sources and energy storage. The proposed framework provides distribution system operators with a computationally efficient and practical tool that allows them to exploit the capabilities of distributed energy resources while maintaining system security and economic efficiency.

Keywords Convex optimization; Battery energy storage scheduling; Active-reactive power dispatch; Degradation cost minimization; Mixed-integer second-order cone programming; Active distribution networks

AMS 2010 subject classifications 46N10

DOI: 10.19139/soic-2310-5070-4311

*Correspondence to: O. D. Montoya (Email: odmontoyag@udistrital.edu.co). Facultad de Ingeniería, Universidad Distrital Francisco José de Caldas, Bogotá D.C. 110121, Colombia.

ISSN 2310-5070 (online) ISSN 2311-004X (print)
Copyright © 2026 International Academic Press

Load Parameters

Nomenclature

Acronyms

ADN Active Distribution Network

BESS Battery Energy Storage System

CG Conventional Generator

CVX MATLAB Modeling System for Convex Optimization

DER Distributed Energy Resource

MINLP Mixed-Integer Nonlinear Program

MISOCP Mixed-Integer Second-Order Cone Program

MPPT Maximum Power Point Tracking

O&M Operation and Maintenance

PV Photovoltaic

SoC State of Charge

SOCP Second-Order Cone Program

Objective Function

F Total daily operational cost [USD/day]

F_{BESS} BESS operation and maintenance cost [USD/day]

F_{deg} Battery degradation cost [USD/day]

F_{energy} Energy procurement cost [USD/day]

F_{PV} PV operation and maintenance cost [USD/day]

Parameters

β^{loss} Power loss factor accounting for network losses [p.u.]

β^{Q} Reactive power penalty factor [p.u.]

Δt Duration of each time interval [h]

η_b^{ch} Charging efficiency of BESS b [p.u.]

η_b^{dis} Discharging efficiency of BESS b [p.u.]

λ_t Energy price at time t [USD/MWh]

$\text{SoC}_b^{\max}$ Maximum state-of-charge limit of BESS b [p.u.]

$\text{SoC}_b^{\min}$ Minimum state-of-charge limit of BESS b [p.u.]

$\mathrm{SoC}_b^{\text{fin}}$ Final state-of-charge of BESS b at the end of the horizon [p.u.]

$\mathrm{SoC}_b^{\text{ini}}$ Initial state-of-charge of BESS b at the beginning of the horizon [p.u.]

$\rho_{i,t}$ Normalized irradiance profile for PV generator i at time t [p.u.]

σ_b Self-discharge rate of BESS b [p.u./h]

$C_{\text{O\&M}}^{\text{BESS}}$ Operation and maintenance cost for BESS operation [USD/MWh]

C^{deg} Degradation cost coefficient [USD/cycle]

$C_{\text{O\&M}}^{\text{PV}}$ Operation and maintenance cost for PV generation [USD/MWh]

E_b Energy capacity of BESS b [MWh]

$P_b^{\text{ch,max}}$ Maximum charging power of BESS b [MW]

$P_b^{\text{dis,max}}$ Maximum discharging power of BESS b [MW]

P_i^{rated} Rated active power of PV generator i [MW]

P_t^d Active power demand at time t [p.u.]

Q_t^d Reactive power demand at time t [p.u.]

S_b^{inv} Apparent power rating of BESS inverter b [MVA]

S_i^{inv} Apparent power rating of PV inverter i [MVA]

T Number of time intervals in the scheduling horizon

Sets

$\mathcal{B}$ Set of battery energy storage systems, $\mathcal{B} = \{1, 2, \ldots, N_{\text{BESS}}\}$

$\mathcal{P}$ Set of photovoltaic generators, $\mathcal{P} = \{1, 2, \ldots, N_{\text{PV}}\}$

$\mathcal{T}$ Set of time intervals, $\mathcal{T} = \{1, 2, \ldots, T\}$

Variables

$\mathrm{SoC}_{b,t}$ State-of-charge of BESS b at time t [p.u.]

$P_{b,t}^{\text{ch}}$ Charging power of BESS b at time t [MW], negative or zero

$P_{b,t}^{\text{dis}}$ Discharging power of BESS b at time t [MW], positive or zero

$P_{i,t}^{\text{PV}}$ Active power output of PV generator i at time t [MW]

P_t^g Active power injection from the substation at time t [MW]

$Q_{b,t}^{\text{BESS}}$ Reactive power output of BESS b at time t [MVAr]

$Q_{i,t}^{\text{PV}}$ Reactive power output of PV generator i at time t [MVAr]

Q_t^g Reactive power injection from the substation at time t [MVAr]

$S_t^g = P_t^g + jQ_t^g$ Complex power injection from the substation at time t [MVA]

$x_{b,t}^{\text{ch}}$ Binary variable equal to 1 if BESS b is charging at time t

$x_{b,t}^{\text{dis}}$ Binary variable equal to 1 if BESS b is discharging at time t

1. Introduction

The global energy landscape is undergoing a profound transformation driven by the urgent need to decarbonize electricity generation, enhance energy security, and modernize aging infrastructure [1, 2]. This transition has driven an unprecedented proliferation of distributed energy resources (DERs), particularly renewable generation such as photovoltaic (PV) systems and flexible assets such as battery energy storage systems (BESS) [3]. Although these technologies offer significant environmental and operational benefits, integrating them into traditional distribution networks—originally designed for unidirectional power flow from centralized generation to passive loads—poses substantial technical and economic challenges that require advanced planning and operational tools [2, 4].

Among the various DER technologies, BESS has emerged as a particularly versatile and valuable asset for active distribution networks (ADNs). By providing capabilities such as energy arbitrage, peak shaving, load shifting, frequency regulation, and voltage support, BESS can significantly enhance the operational flexibility and economic efficiency of distribution systems [5, 6]. Furthermore, modern BESS inverters are capable of independently controlling both active and reactive power within their apparent power limits, enabling them to provide multiple grid services simultaneously [7]. However, the effective utilization of these capabilities requires sophisticated optimization frameworks that can coordinate the dispatch of multiple BESS units while accounting for the full AC network physics, operational constraints, and economic factors such as battery degradation [8].

Despite the growing body of literature on BESS scheduling and optimization, several critical research gaps persist that motivate the present work. First, the vast majority of existing approaches treat active and reactive power dispatch as decoupled problems, failing to exploit the full capability of modern BESS inverters to provide coordinated active-reactive support [6, 9]. This decoupling not only limits the economic benefits of BESS operation but also overlooks the potential for reactive power support to mitigate voltage issues and reduce network losses, a capability that is increasingly recognized as essential for modern distribution systems [7, 10]. Second, battery degradation—arguably the most significant economic factor influencing BESS operational decisions—is frequently modeled using oversimplified representations, such as linear functions of energy throughput or simplistic cycle counting, without adequately capturing the complex interdependencies among depth-of-discharge, state-of-charge, and temperature effects [3, 11]. While recent studies have begun to incorporate more sophisticated degradation models, many still rely on simplified cycle counting approaches that do not fully capture the nonlinear nature of battery aging [12]. Third, many existing formulations rely on linearized or approximated power flow models, such as DC power flow or second-order cone programming relaxations, which may fail to accurately capture the full AC network physics essential for operational feasibility [7, 13]. This limitation is particularly problematic for distribution networks characterized by high R/X ratios, where active and reactive power flows exhibit strong coupling and voltage-constrained operation is critical to system security and power quality [14]. Furthermore, while uncertainty management approaches for active distribution system planning have received considerable attention [4], the integration of degradation-aware BESS scheduling with coordinated active-reactive dispatch under realistic AC network constraints remains an open challenge [10, 15]. The growing complexity of modern distribution systems, driven by the global renewable energy transition and the proliferation of DERs [1, 2], demands integrated optimization frameworks that simultaneously address these interrelated challenges.

To clearly position the contribution of this work with respect to the existing literature, Table 1 provides a comparative analysis of recent BESS scheduling frameworks across six key features: stochastic uncertainty modeling, battery degradation modeling, reactive power coordination, convex reformulation, exactness of the reformulation, and multi-scenario capability. As shown in Table 1, although previous studies have addressed some of these features individually, none of them combines all of them within a single tractable formulation. For instance, while some works incorporate stochastic uncertainty modeling [3, 4], they often rely on simplified degradation models or do not consider reactive power coordination. Conversely, studies that address reactive power capabilities [7, 9] may not include detailed degradation cost models or may use relaxations that are not exact. The proposed framework is the only one that simultaneously integrates stochastic uncertainty modeling (through scenario-based analysis), detailed battery degradation modeling via equivalent full-cycle counting, coordinated active-reactive power dispatch, convex reformulation via MISOCP, exactness of the reformulation (no relaxation error), and multi-scenario capability, thereby offering a comprehensive and computationally efficient solution for day-ahead BESS scheduling in active distribution networks.

Table 1. Comparative analysis of recent BESS scheduling frameworks.

Reference	Stochastic Uncertainty	Degradation Modeling	Reactive Power	Convex Reform.	Exact Reform.	Multi-Scenario
[6]	No	Simplified	No	No	–	No
[7]	Yes	Simplified	Yes	Yes	No	No
[9]	Yes	Simplified	Yes	Yes	No	No
[11]	No	Detailed	No	No	–	No
[3]	Yes	Simplified	No	No	–	No
[12]	No	Simplified	No	No	–	No
[13]	Yes	Detailed	No	No	–	No
[10]	Yes	Simplified	Yes	No	–	No
[15]	Yes	Simplified	No	No	–	No
[16]	No	Detailed	No	No	–	No
[17]	No	Detailed	No	No	–	No
This work	**Yes**	**Detailed**	**Yes**	**Yes**	**Yes**	**Yes**

The proposed framework makes several key contributions to the existing literature. First, we formulate a comprehensive mixed-integer nonlinear programming model that simultaneously optimizes the coordinated active and reactive power dispatch of BESS and PV units while enforcing the power balance equation at each time interval for an aggregated single-node representation of the distribution network. Unlike most existing approaches that treat active and reactive power independently, our formulation exploits the inverter capabilities of modern DERs, enabling BESS units to provide both energy arbitrage and reactive power support services at the same time. Second, we incorporate a detailed battery degradation cost model using an equivalent full-cycle counting approach based on the cumulative variation of the state-of-charge trajectory. This model captures the economic impact of cycling on battery lifetime, enabling the optimization to balance short-term operational revenues against long-term asset preservation. Third, we demonstrate that the resulting MINLP can be exactly reformulated as a mixed-integer second-order cone program through the convex reformulation of the apparent power constraints and the linearization of the absolute value terms in the degradation cost. This reformulation preserves convexity and allows the problem to be solved efficiently using state-of-the-art optimization solvers, making it suitable for day-ahead operational planning. Fourth, the aggregated single-node representation provides a computationally efficient framework that focuses on the energy-time dimension of the problem—specifically, the optimal charging and discharging patterns, energy arbitrage opportunities, and the economic trade-offs between operational revenues and battery degradation. Although this approach does not capture voltage profiles or branch power flows, it offers valuable insights for preliminary feasibility studies and parametric analyses, enabling rapid assessment of BESS economic viability under different price scenarios and load profiles. The reactive power support provided by the DERs is modeled as a reduction in reactive power procurement from the substation, which indirectly contributes to loss reduction and improved network efficiency.

The proposed framework is implemented using MATLAB CVX with the Gurobi solver, providing a practical and computationally efficient tool for distribution system operators. The methodology is validated on a modified 33-bus radial distribution network incorporating three PV generation units and three BESS units, with detailed time-varying load profiles, solar irradiance profiles, and energy price data representing realistic Colombian distribution system conditions [18]. The computational analysis is organized around seven distinct scenarios that progressively introduce distributed energy resources and reactive power control capabilities, allowing a comprehensive evaluation of their individual and combined impacts on the network operational costs.

The remainder of this paper is organized as follows. Section 2 presents the complete mathematical formulation of the optimization problem, including the objective function components and all operational constraints. Section 3 describes the convex reformulation of the MINLP into an MISOCP and the implementation details using MATLAB CVX with the Gurobi solver. Section 4 provides a detailed description of the test system, including network topology, line parameters, load profiles, PV generation data, BESS characteristics, and economic parameters. Section 5 presents and discusses the computational results obtained from the seven scenarios, demonstrating the progressive benefits of integrating distributed energy resources and enabling reactive power control. Finally, Section 6 concludes the paper by summarizing the main findings and outlining directions for future research.

2. Mathematical Formulation of the Optimal Battery Management Problem

This section presents a comprehensive MINLP model for the optimal scheduling of BESS in active distribution networks. The formulation employs an aggregated single-node representation of the distribution network, where all loads, generators, and storage devices are connected to a common substation (slack bus) [16]. Although this simplification does not capture detailed voltage profiles or branch power flows, it provides a computationally efficient framework for studying the economic and operational aspects of BESS integration while capturing the essential physical constraints and economic trade-offs inherent in real-world distribution systems [19].

The scheduling horizon is discretized into T intervals of equal duration Δt (typically one hour), with $t \in \mathcal{T} = \{1, 2, \ldots, T\}$. The network comprises N_{PV} photovoltaic generators indexed by $i \in \mathcal{P} = \{1, 2, \ldots, N_{\text{PV}}\}$ and N_{BESS} battery energy storage systems indexed by $b \in \mathcal{B} = \{1, 2, \ldots, N_{\text{BESS}}\}$.

The optimization problem determines the following decision variables: the complex power injection from the substation $S_t^g = P_t^g + jQ_t^g$ at each time interval; the active power output of each PV generator $P_{i,t}^{\text{PV}}$; the charging power $P_{b,t}^{\text{ch}}$ (negative or zero) and discharging power $P_{b,t}^{\text{dis}}$ (positive or zero) of each BESS; the reactive power output of each BESS $Q_{b,t}^{\text{BESS}}$; and the state-of-charge $\text{SoC}_{b,t}$ of each battery. In addition, binary variables $x_{b,t}^{\text{ch}}$ and $x_{b,t}^{\text{dis}}$ indicate whether a BESS is charging or discharging at each time interval, respectively.

2.1. *Objective Function*

The objective is to minimize the total daily operational cost F, which comprises four components: the cost of energy procurement from the substation, the operation and maintenance cost of PV generation, the operation and maintenance cost of BESS operation, and the cost associated with battery degradation due to cycling [20].

2.1.1. Energy Procurement Cost The energy procurement cost represents the expense of purchasing active and reactive power from the upstream grid through the substation. In real distribution systems, the power delivered to end-users experiences losses along the feeders, requiring additional energy to be purchased from the substation to meet the actual load demand [21]. These losses are modelled through a loss factor β^{loss} (typically set to 3% in distribution networks), which multiplies the active power purchased. Similarly, the flow of reactive power contributes to additional losses and voltage drops, which is captured through a penalty factor β^{Q} (typically 20% of the active power cost) applied to the absolute value of reactive power [22, 23]. The energy procurement cost is therefore expressed as:

$$F_{\text{energy}} = \Delta t \sum_{t=1}^{T} \lambda_t \, P_t^g \left(1 + \beta^{\text{loss}}\right) + \beta^{\text{Q}} \Delta t \sum_{t=1}^{T} \lambda_t \, |Q_t^g|, \tag{1}$$

where λ_t is the time-varying energy price at time t expressed in USD/MWh. This formulation encourages the optimization to minimize both the active and reactive power drawn from the substation, thereby promoting efficient operation of the distribution system.

2.1.2. PV Operation and Maintenance Cost The operation and maintenance (O&M) cost of PV generation accounts for the variable maintenance expenses associated with operating photovoltaic systems, including cleaning, inspection, and minor repairs [24, 25]. This cost is assumed to be directly proportional to the total energy produced by the PV generators over the horizon:

$$F_{\text{PV}} = C_{\text{O\&M}}^{\text{PV}} \Delta t \sum_{t=1}^{T} \sum_{i=1}^{N_{\text{PV}}} P_{i,t}^{\text{PV}}, \tag{2}$$

where $C_{\text{O\&M}}^{\text{PV}}$ is the unit O&M cost expressed in USD/MWh. Since this term is minimized, the optimization inherently favours the utilization of PV generation to offset energy purchases from the substation, as long as the cost of PV O&M is lower than the energy price at that time interval [8].

2.1.3. BESS Operation and Maintenance Cost The O&M cost of BESS operation accounts for the wear and maintenance associated with charging and discharging cycles. This cost is proportional to the absolute power exchanged between the battery and the network, reflecting that both charging and discharging contribute to the operational stress on the battery system [20]:

$$F_{\text{BESS}} = C_{\text{O\&M}}^{\text{BESS}} \Delta t \sum_{t=1}^{T} \sum_{b=1}^{N_{\text{BESS}}} \left(P_{b,t}^{\text{ch}} + P_{b,t}^{\text{dis}} \right), \tag{3}$$

where $C_{\text{O\&M}}^{\text{BESS}}$ is the unit O&M cost for BESS operation in USD/MWh. The term $\left(P_{b,t}^{\text{ch}} + P_{b,t}^{\text{dis}} \right)$ represents the absolute power throughput, since $P_{b,t}^{\text{ch}} \leq 0$ and $P_{b,t}^{\text{dis}} \geq 0$. This formulation discourages unnecessary battery cycling and promotes a more conservative operational strategy when the economic benefits do not justify the associated wear.

2.1.4. Battery Degradation Cost Battery degradation is one of the most significant economic factors influencing BESS operational decisions. The capacity of a battery decreases over time due to cycling (charge and discharge events), with the rate of degradation strongly influenced by the depth and frequency of cycles [26]. To capture this effect, the degradation cost is modelled using an equivalent full-cycle counting approach based on the cumulative variation of the state-of-charge trajectory [17]:

$$F_{\text{deg}} = C^{\text{deg}} \sum_{b=1}^{N_{\text{BESS}}} \left(\frac{1}{2} \sum_{t=2}^{T} |\text{SoC}_{b,t} - \text{SoC}_{b,t-1}| + \frac{1}{2} \left| \text{SoC}_{b,1} - \text{SoC}_{b}^{\text{ini}} \right| \right), \tag{4}$$

where C^{deg} is the degradation cost coefficient in USD per equivalent full cycle. The first term $\frac{1}{2} \sum_{t=2}^{T} |\text{SoC}_{b,t} - \text{SoC}_{b,t-1}|$ counts half-cycles based on the cumulative absolute variation of the SoC over the horizon. The second term $\frac{1}{2}|\text{SoC}_{b,1} - \text{SoC}_{b}^{\text{ini}}|$ accounts for the initial half-cycle from the initial SoC at the beginning of the horizon to the SoC at the first time interval. The factor of $1/2$ converts these half-cycles to equivalent full cycles, providing a reasonable approximation of the degradation induced by the operational schedule. This formulation effectively penalizes excessive cycling, encouraging the optimization to smooth the SoC trajectory and reduce the depth of discharge where economically justified.

2.1.5. Complete Objective Function The total daily operational cost is the sum of the four components described above:

$$\boxed{\min \quad F = F_{\text{energy}} + F_{\text{PV}} + F_{\text{BESS}} + F_{\text{deg}}} \tag{5}$$

This multi-term objective captures the key economic drivers of BESS operation and provides a comprehensive framework for evaluating operational strategies that balance short-term energy arbitrage opportunities against long-term battery life considerations.

2.2. Operational Constraints

The optimization is subject to a comprehensive set of operational and physical constraints that ensure technical feasibility and safe operation of the distribution system and its components. These constraints are organized by the type of device or system they govern.

2.2.1. Photovoltaic Generator Constraints PV generators are dispatched according to daily demand requirements and grid operational needs, rather than strictly following maximum power point tracking (MPPT) conditions [27]. This means that the active power output can be curtailed or adjusted to maintain system balance and economic efficiency. The active power output of each PV generator is bounded between zero and the available power, which is determined by the rated capacity and the normalized irradiance profile at that time:

$$0 \leq P_{i,t}^{\text{PV}} \leq P_i^{\text{rated}} \rho_{i,t}, \quad \forall i, t, \tag{6}$$

where $\rho_{i,t} \in [0, 1]$ represents the fraction of rated power available from the solar resource at time t. The upper bound represents the maximum power that could be generated, but the optimization may choose any value below this limit based on economic and operational considerations.

Unlike traditional MPPT operation, which fixes reactive power at zero, the proposed framework allows PV inverters to provide reactive power support within their apparent power capability. This enables PV generators to operate at variable power factors, contributing to reactive power compensation and loss reduction. The reactive power output of each PV generator is therefore a decision variable bounded by the inverter's apparent power rating:

$$\left|Q_{i,t}^{\text{PV}}\right| \leq \sqrt{\left(S_i^{\text{inv}}\right)^2 - \left(P_{i,t}^{\text{PV}}\right)^2}, \quad \forall i, t, \tag{7}$$

where S_i^{inv} is the apparent power rating of the PV inverter in MVA. This constraint ensures that the inverter operates within its thermal and electrical limits while allowing flexibility to provide reactive power support when economically beneficial.

The complex power output of each PV generator is expressed as:

$$S_{i,t}^{\text{PV}} = P_{i,t}^{\text{PV}} + jQ_{i,t}^{\text{PV}}, \quad \forall i, t. \tag{8}$$

2.2.2. Battery Energy Storage System Constraints The BESS operational constraints represent the most complex set of restrictions in the formulation, governing the power limits, mode of operation, apparent power capability, state-of-charge dynamics, and SoC limits of each battery [7, 19].

Power Limits. The charging and discharging powers are bounded by the converter's rated limits, with the binary variables enforcing that power can only flow in the direction permitted by the selected operational mode:

$$P_b^{\text{ch,max}} x_{b,t}^{\text{ch}} \leq P_{b,t}^{\text{ch}} \leq 0, \quad \forall b, t, \tag{9}$$

$$0 \leq P_{b,t}^{\text{dis}} \leq P_b^{\text{dis,max}} x_{b,t}^{\text{dis}}, \quad \forall b, t, \tag{10}$$

where $P_b^{\text{ch,max}}$ is a negative number representing the maximum charging power (i.e., the most negative value allowed), and $P_b^{\text{dis,max}}$ is a positive number representing the maximum discharging power. The binary variables $x_{b,t}^{\text{ch}}$ and $x_{b,t}^{\text{dis}}$ take values of 0 or 1. If $x_{b,t}^{\text{ch}} = 1$, the charging power $P_{b,t}^{\text{ch}}$ can take values between $P_b^{\text{ch,max}}$ and 0 (i.e., the battery can charge up to its maximum rate), while the discharging power $P_{b,t}^{\text{dis}}$ is forced to zero. Conversely, if $x_{b,t}^{\text{dis}} = 1$, the discharging power can take values between 0 and $P_b^{\text{dis,max}}$, while the charging power is forced to zero.

Exclusive Mode Constraint. A BESS cannot charge and discharge simultaneously, as this would create internal power circulation that reduces overall efficiency, increases wear, and represents an economically suboptimal mode of operation [19]. This exclusivity is enforced by:

$$x_{b,t}^{\text{ch}} + x_{b,t}^{\text{dis}} = 1, \quad \forall b, t. \tag{11}$$

This constraint ensures that exactly one of the binary variables is equal to 1 at each time interval, meaning the battery is either charging or discharging, but not both.

Apparent Power Limit. The BESS inverter is rated for a maximum apparent power S_b^{inv}, which limits the combination of active and reactive power that can be exchanged with the network [6]. This constraint is expressed as:

$$\left(P_{b,t}^{\text{ch}} + P_{b,t}^{\text{dis}}\right)^2 + \left(Q_{b,t}^{\text{BESS}}\right)^2 \leq \left(S_b^{\text{inv}}\right)^2, \quad \forall b, t. \tag{12}$$

This quadratic constraint ensures that the inverter does not exceed its thermal capacity, regardless of the power factor at which the battery operates. The term $\left(P_{b,t}^{\text{ch}} + P_{b,t}^{\text{dis}}\right)$ represents the net active power output of the battery (positive for discharge, negative for charge), and $Q_{b,t}^{\text{BESS}}$ is the reactive power output. This constraint couples the active and reactive power decisions, reflecting the physical limitations of the power electronic converter.

State-of-Charge Dynamics. The evolution of the state-of-charge over time is governed by the energy balance equation, which accounts for self-discharge and the conversion efficiencies of charging and discharging [19]:

$$\text{SoC}_{b,t} = (1 - \sigma_b \Delta t)\,\text{SoC}_{b,t-1} - \frac{\Delta t}{E_b}\left(\eta_b^{\text{ch}} P_{b,t}^{\text{ch}} + \frac{1}{\eta_b^{\text{dis}}} P_{b,t}^{\text{dis}}\right), \quad \forall b, t, \tag{13}$$

with the convention that $P_{b,t}^{\text{ch}} \leq 0$ and $P_{b,t}^{\text{dis}} \geq 0$. The term $(1 - \sigma_b \Delta t)$ is the self-retention factor, representing the fraction of energy retained after accounting for self-discharge over the interval Δt. The parameter σ_b is the self-discharge rate per hour, typically around 0.002 (0.2%) for lithium-ion batteries. The factor $\Delta t / E_b$ converts the power terms to changes in SoC, where E_b is the energy capacity of the battery in MWh. The charging efficiency η_b^{ch} multiplies the charging power (which is negative), effectively reducing the amount of energy stored in the battery relative to the energy drawn from the network. The discharging efficiency η_b^{dis} divides the discharging power, meaning that more energy must be taken from the battery than is delivered to the network to account for internal losses.

State-of-Charge Limits. To prevent overcharging and deep discharge, which would accelerate degradation and pose safety risks, the SoC must remain within specified minimum and maximum limits [20]:

$$\text{SoC}_b^{\min} \leq \text{SoC}_{b,t} \leq \text{SoC}_b^{\max}, \quad \forall b, t. \tag{14}$$

These limits are typically set between 0.10 and 0.90 for lithium-ion batteries, although the specific values depend on the battery chemistry and the manufacturer's recommendations. Operating within these limits is essential for maintaining battery health and ensuring safe operation.

Boundary Conditions. The initial and final SoC are fixed to ensure that the BESS is returned to a specified state at the beginning and end of the horizon, enabling daily cyclic operation and preventing the optimization from depleting or overcharging the battery at the boundaries:

$$\text{SoC}_{b,0} = \text{SoC}_b^{\text{ini}}, \quad \forall b, \tag{15}$$

$$\text{SoC}_{b,T} = \text{SoC}_b^{\text{fin}}, \quad \forall b. \tag{16}$$

The initial SoC $\text{SoC}_b^{\text{ini}}$ represents the state of the battery at the start of the day, while the final SoC $\text{SoC}_b^{\text{fin}}$ represents the desired state at the end of the day. Typically, these values are set equal to ensure cyclic operation, but they can be different if the operator intends to charge or discharge the battery over the course of the day.

2.2.3. Power Balance Constraint At each time interval, the total complex power injected into the system must equal the total load demand, ensuring that the system is in equilibrium at all times:

$$S_t^g + \sum_{i=1}^{N_{\text{PV}}} P_{i,t}^{\text{PV}} + \sum_{b=1}^{N_{\text{BESS}}} \left(P_{b,t}^{\text{ch}} + P_{b,t}^{\text{dis}} + jQ_{b,t}^{\text{BESS}}\right) = P_t^d + jQ_t^d, \quad \forall t. \tag{17}$$

This equation expresses that the sum of all power injections from the substation, PV generators, and BESS units equals the total load demand at each time interval. The load demand $P_t^d + jQ_t^d$ is assumed to be known from historical data or forecasts and includes both active and reactive components.

2.2.4. Substation Power Limits The substation has physical and contractual limits on the power it can inject into the distribution system. The real power injection is constrained to be non-negative, meaning that the substation cannot operate as a load (i.e., cannot absorb power from the network):

$$P_t^g \geq 0, \quad \forall t. \tag{18}$$

Similarly, the reactive power injection is constrained to be non-negative, preventing reverse reactive power flow that could cause voltage rise or other operational issues:

$$Q_t^g \geq 0, \quad \forall t. \tag{19}$$

2.3. Compact Problem Statement

The complete optimization problem is summarized as:

$$\boxed{\begin{array}{ll}
\min & F = F_{\text{energy}} + F_{\text{PV}} + F_{\text{BESS}} + F_{\text{deg}} \\
\text{s.t.} & 0 \leq P_{i,t}^{\text{PV}} \leq P_i^{\text{rated}} \rho_{i,t}, \ \left|Q_{i,t}^{\text{PV}}\right| \leq \sqrt{(S_i^{\text{inv}})^2 - (P_{i,t}^{\text{PV}})^2}, \quad \forall i, t, \\
& P_b^{\text{ch,max}} x_{b,t}^{\text{ch}} \leq P_{b,t}^{\text{ch}} \leq 0, \ 0 \leq P_{b,t}^{\text{dis}} \leq P_b^{\text{dis,max}} x_{b,t}^{\text{dis}}, \quad \forall b, t, \\
& x_{b,t}^{\text{ch}} + x_{b,t}^{\text{dis}} = 1, \quad \forall b, t, \\
& \left(P_{b,t}^{\text{ch}} + P_{b,t}^{\text{dis}}\right)^2 + \left(Q_{b,t}^{\text{BESS}}\right)^2 \leq \left(S_b^{\text{inv}}\right)^2, \quad \forall b, t, \\
& \text{SoC}_{b,t} = (1 - \sigma_b \Delta t)\text{SoC}_{b,t-1} - \dfrac{\Delta t}{E_b}\left(\eta_b^{\text{ch}} P_{b,t}^{\text{ch}} + \dfrac{1}{\eta_b^{\text{dis}}} P_{b,t}^{\text{dis}}\right), \quad \forall b, t, \\
& \text{SoC}_b^{\min} \leq \text{SoC}_{b,t} \leq \text{SoC}_b^{\max}, \quad \forall b, t, \\
& \text{SoC}_{b,0} = \text{SoC}_b^{\text{ini}}, \ \text{SoC}_{b,T} = \text{SoC}_b^{\text{fin}}, \quad \forall b, \\
& S_t^g + \displaystyle\sum_i S_{i,t}^{\text{PV}} + \sum_b \left(P_{b,t}^{\text{ch}} + P_{b,t}^{\text{dis}} + jQ_{b,t}^{\text{BESS}}\right) = P_t^d + jQ_t^d, \quad \forall t, \\
& P_t^g \geq 0, \ Q_t^g \geq 0, \quad \forall t, \\
& x_{b,t}^{\text{ch}}, x_{b,t}^{\text{dis}} \in \{0, 1\}.
\end{array}}$$

3. Solution Methodology

The optimization model formulated in the previous section is a mixed-integer nonlinear program (MINLP) that presents computational challenges due to the presence of binary variables, the nonlinear apparent power constraint, and the absolute value terms in the degradation cost. This section describes the convex reformulation that renders the problem tractable using modern optimization solvers, followed by the implementation details using MATLAB CVX with the Gurobi solver. The solution methodology follows a structured three-stage workflow: data processing and normalization, problem formulation and solution within CVX, and extraction and analysis of the optimal results.

3.1. Convex Reformulation

The problem structure allows for a reformulation that transforms the MINLP into a mixed-integer second-order cone program (MISOCP), which is efficiently solvable by state-of-the-art optimization solvers.

3.1.1. Second-Order Cone Reformulation of Apparent Power Constraints The quadratic apparent power constraint (12) is the primary source of nonlinearity in the continuous relaxation of the problem. However, this constraint can be exactly reformulated as a second-order cone constraint:

$$\left\| \begin{bmatrix} P^{\text{ch}}_{b,t} + P^{\text{dis}}_{b,t} \\ Q^{\text{BESS}}_{b,t} \end{bmatrix} \right\|_2 \leq S^{\text{inv}}_b, \quad \forall b, t, \tag{20}$$

where $\|\cdot\|_2$ denotes the Euclidean norm. This reformulation is exact: the quadratic constraint and its second-order cone representation define the same feasible set, so no relaxation or approximation error is introduced. This exactness is fundamental to the proposed methodology, as it guarantees that the solution of the MISOCP is also a feasible and globally optimal solution of the original MINLP. This reformulation preserves the convexity of the continuous relaxation and allows the problem to be solved as a MISOCP, for which efficient polynomial-time interior-point algorithms exist.

3.1.2. Linearization of Absolute Value Terms The degradation cost (4) contains absolute value terms that introduce nondifferentiability and nonlinearity into the objective function. These terms can be linearized by introducing auxiliary variables and additional constraints, which maintains the convexity of the continuous relaxation.

For the term $|\text{SoC}_{b,t} - \text{SoC}_{b,t-1}|$, we introduce a non-negative auxiliary variable $z_{b,t} \geq 0$ and impose the following constraints:

$$z_{b,t} \geq \text{SoC}_{b,t} - \text{SoC}_{b,t-1}, \quad \forall b, t = 2, \ldots, T, \tag{21}$$

$$z_{b,t} \geq \text{SoC}_{b,t-1} - \text{SoC}_{b,t}, \quad \forall b, t = 2, \ldots, T. \tag{22}$$

Similarly, for the initial half-cycle term $\left|\text{SoC}_{b,1} - \text{SoC}^{\text{ini}}_b\right|$, we introduce an auxiliary variable $z_{b,1} \geq 0$ with:

$$z_{b,1} \geq \text{SoC}_{b,1} - \text{SoC}^{\text{ini}}_b, \quad \forall b, \tag{23}$$

$$z_{b,1} \geq \text{SoC}^{\text{ini}}_b - \text{SoC}_{b,1}, \quad \forall b. \tag{24}$$

The objective function is then modified to use the auxiliary variables:

$$F_{\text{deg}} = C^{\text{deg}} \sum_{b=1}^{N_{\text{BESS}}} \left(\frac{1}{2} \sum_{t=2}^{T} z_{b,t} + \frac{1}{2} z_{b,1} \right). \tag{25}$$

This linearization is exact because the constraints (21)–(22) force $z_{b,t}$ to be at least the absolute difference, and since the objective function minimizes $z_{b,t}$, it will take exactly the value of the absolute difference at the optimum. In other words, at optimality, the auxiliary variables satisfy $z_{b,t} = |\text{SoC}_{b,t} - \text{SoC}_{b,t-1}|$ and $z_{b,1} = |\text{SoC}_{b,1} - \text{SoC}^{\text{ini}}_b|$, so the degradation cost is represented exactly. This property, combined with the exact second-order cone reformulation of the apparent power constraints, ensures that the resulting MISOCP is an equivalent reformulation of the original MINLP, preserving both the feasible set and the optimal objective value. Consequently, the schedule obtained from the MISOCP is globally optimal for the original problem.

3.1.3. Resulting MISOCP Formulation After applying these reformulations, the original MINLP is transformed into the following MISOCP problem:

$$\boxed{\begin{array}{ll}
\min & F = F_{\text{energy}} + F_{\text{PV}} + F_{\text{BESS}} + F_{\text{deg}}^{\text{lin}} \\
\text{s.t.} & 0 \leq P_{i,t}^{\text{PV}} \leq P_i^{\text{rated}} \rho_{i,t}, \ \left|Q_{i,t}^{\text{PV}}\right| \leq \sqrt{(S_i^{\text{inv}})^2 - (P_{i,t}^{\text{PV}})^2}, \quad \forall i, t, \\
& P_b^{\text{ch,max}} x_{b,t}^{\text{ch}} \leq P_{b,t}^{\text{ch}} \leq 0, \ 0 \leq P_{b,t}^{\text{dis}} \leq P_b^{\text{dis,max}} x_{b,t}^{\text{dis}}, \quad \forall b, t, \\
& x_{b,t}^{\text{ch}} + x_{b,t}^{\text{dis}} = 1, \quad \forall b, t, \\
& \left\| \begin{bmatrix} P_{b,t}^{\text{ch}} + P_{b,t}^{\text{dis}} \\ Q_{b,t}^{\text{BESS}} \end{bmatrix} \right\|_2 \leq S_b^{\text{inv}}, \quad \forall b, t, \quad \text{(SOCP constraint)} \\
& \text{SoC}_{b,t} = (1 - \sigma_b \Delta t)\text{SoC}_{b,t-1} - \dfrac{\Delta t}{E_b} \left(\eta_b^{\text{ch}} P_{b,t}^{\text{ch}} + \dfrac{1}{\eta_b^{\text{dis}}} P_{b,t}^{\text{dis}} \right), \quad \forall b, t, \\
& \text{SoC}_b^{\min} \leq \text{SoC}_{b,t} \leq \text{SoC}_b^{\max}, \quad \forall b, t, \\
& \text{SoC}_{b,0} = \text{SoC}_b^{\text{ini}}, \ \text{SoC}_{b,T} = \text{SoC}_b^{\text{fin}}, \quad \forall b, \\
& S_t^g + \sum_i \left(P_{i,t}^{\text{PV}} + jQ_{i,t}^{\text{PV}} \right) + \sum_b \left(P_{b,t}^{\text{ch}} + P_{b,t}^{\text{dis}} + jQ_{b,t}^{\text{BESS}} \right) = P_t^d + jQ_t^d, \quad \forall t, \\
& P_t^g \geq 0, \ Q_t^g \geq 0, \quad \forall t, \\
& z_{b,t} \geq \text{SoC}_{b,t} - \text{SoC}_{b,t-1}, \ z_{b,t} \geq \text{SoC}_{b,t-1} - \text{SoC}_{b,t}, \quad \forall b, t = 2, \ldots, T, \\
& z_{b,1} \geq \text{SoC}_{b,1} - \text{SoC}_b^{\text{ini}}, \ z_{b,1} \geq \text{SoC}_b^{\text{ini}} - \text{SoC}_{b,1}, \quad \forall b, \\
& x_{b,t}^{\text{ch}}, x_{b,t}^{\text{dis}} \in \{0, 1\}, \quad z_{b,t} \geq 0.
\end{array}}$$

The reformulated MISOCP preserves the convexity of the continuous relaxation while representing the original nonlinear constraints exactly. The apparent power constraints for both PV and BESS inverters are expressed as second-order cone constraints, which are computationally tractable and can be efficiently solved using interior-point methods. The linearization of the absolute value terms in the degradation cost introduces auxiliary variables $z_{b,t}$ that exactly represent the absolute differences in the SoC trajectory without introducing approximation errors.

This reformulation allows the problem to be solved with state-of-the-art MISOCP solvers such as Gurobi, CPLEX, or MOSEK, which can handle large-scale problems with thousands of variables and constraints. The computational efficiency of this approach makes it suitable for day-ahead operational planning, where the optimization must be solved within reasonable time frames, typically requiring less than 10 seconds for a 24-hour horizon with three BESS units and three PV units.

Remark 1

The PV reactive power constraint $\left|Q_{i,t}^{\text{PV}}\right| \leq \sqrt{(S_i^{\text{inv}})^2 - (P_{i,t}^{\text{PV}})^2}$ is nonlinear but can be reformulated as a second-order cone constraint for the MISOCP formulation. However, in the compact problem statement above, it is presented in its original form for clarity. In practice, this constraint can be implemented directly in CVX using the `norm()` function with appropriate variables.

3.2. MATLAB CVX Implementation

The reformulated MISOCP problem is implemented using MATLAB CVX, a modeling system for convex optimization that provides a high-level interface for specifying and solving disciplined convex programs [28]. The Gurobi solver is selected due to its efficient handling of mixed-integer second-order cone programs.

The solution methodology follows a structured three-stage workflow:

1. **Data Processing and Normalization:** All quantities are converted to the per-unit system, and all time-varying parameters are prepared.

2. **CVX Problem Formulation and Solution:** The problem is specified within CVX using its native syntax, and the Gurobi solver is invoked to solve the resulting MISOCP.
3. **Result Extraction and Analysis:** The optimal solution is extracted from the CVX workspace and analyzed for validation and visualization purposes.

Algorithm 1 summarizes the complete solution procedure, detailing the variable declarations, objective function definition, constraint formulation, and result extraction steps.

Algorithm 1 Solution Methodology Using MATLAB CVX with Gurobi Solver

Input: Network data, load and PV profiles, BESS parameters, economic parameters
Output: Optimal dispatch schedules and total cost
Stage 1: Data Processing
Convert all quantities to per-unit system using base power and base voltage
Compute the available power from each PV generator at each time interval
Compute self-retention factors and SoC conversion factors for each BESS
Aggregate the total complex load demand at each time interval
Prepare all time-varying parameters (load profiles, PV availability, energy prices)
Stage 2: CVX Problem Formulation
`cvx_begin`
`cvx_solver Gurobi`
`cvx_precision best`
Variable Declaration
Declare substation complex power as continuous variables
Declare PV complex power as continuous variables
Declare BESS variables: complex power, charging power, discharging power, reactive power
Declare state-of-charge variables for each BESS as continuous variables
Declare binary variables for charging and discharging mode selection
Declare auxiliary variables for degradation cost linearization
Objective Function
Define energy procurement cost (active power with loss factor and reactive power penalty)
Define PV operation and maintenance cost
Define BESS operation and maintenance cost (proportional to absolute power throughput)
Define battery degradation cost (linearized using auxiliary variables)
Set the objective as the sum of all four cost components
Constraints Definition
for Each time interval t **do**
    for Each PV generator i **do**
        Enforce active power limits between zero and available solar power
        Fix reactive power output to zero (MPPT operation)
        Enforce inverter apparent power limit
    end for
    for Each BESS b **do**
        Enforce charging and discharging power limits based on converter ratings
        Enforce exclusive charging/discharging mode using binary variables
        Enforce apparent power limit using second-order cone constraint
        Model state-of-charge dynamics considering self-discharge and efficiencies
        Enforce state-of-charge limits
        Linearize absolute value terms for degradation cost using auxiliary variables
    end for
    Enforce power balance: substation + PV + BESS = load demand
    Enforce substation active and reactive power limits
end for
Enforce final state-of-charge condition at the end of the horizon
`cvx_end`
Stage 3: Result Extraction
Extract optimal substation active and reactive power dispatch
Extract optimal PV generation schedule
Extract optimal BESS active and reactive power dispatch
Extract optimal state-of-charge trajectory
Compute total daily operational cost and its components
Return: Optimal dispatch schedules and total cost

The proposed solution methodology offers several practical advantages for day-ahead operational planning of BESS in distribution networks. First, the use of CVX with the Gurobi solver ensures that the problem is solved with high numerical precision and computational efficiency, typically requiring less than 10 seconds for a 24-hour horizon with three BESS units [29]. Second, the modular structure of the code allows for easy adaptation to different test systems, including the integration of additional BESS units, PV generators, or modified network configurations. Third, the algorithm handles all the complexities of the original MINLP model through the convex reformulation of the apparent power constraints as second-order cone constraints and the linearization of the absolute value terms in the degradation cost. The resulting solution provides distribution system operators with a comprehensive operational schedule that optimally balances energy procurement, renewable generation utilization, and battery life preservation, ultimately enhancing the economic viability of BESS investments in active distribution networks. The complete MATLAB implementation of this methodology, including the CVX model and result visualization scripts, is provided in the supplementary material [30].

3.3. Remark on Network Modelling

The formulation presented above assumes an aggregated single-node representation of the distribution network, where the substation supplies the total load plus losses, and all distributed generators and storage devices are connected to the same node [19]. Although this simplification enables rapid solution and parametric analysis, it does not capture the spatial distribution of loads and generators, the voltage profile across the network, or the power flows through individual branches.

For more detailed analyses that require consideration of voltage constraints, branch thermal limits, and the location-specific effects of distributed resources, the model can be extended to a multi-node formulation with AC power flow constraints. In such a formulation, the power balance equation (17) would be replaced by the full AC power flow equations at each node, and additional constraints would be imposed on voltage magnitudes and branch currents.

Nevertheless, the single-node formulation serves as a computationally efficient tool for preliminary feasibility studies and provides valuable insights into the economic and operational benefits of BESS integration. It is particularly useful for analyzing the energy-time dimension of the problem, understanding the optimal charging and discharging patterns, and assessing the economic viability of BESS investments under different price scenarios and load profiles. The methodology presented here can be readily extended to multi-node formulations by replacing the power balance constraint with the full AC power flow equations, a topic that will be addressed in future work.

4. Test System and Data Description

This section presents the test system employed to evaluate the proposed optimization framework for BESS scheduling in active distribution networks [8]. The system corresponds to the modified 33-bus radial distribution network, a well-established benchmark in the power systems literature, augmented with photovoltaic generation units and battery energy storage systems. The complete data set, including network topology, line parameters, load profiles, PV generation profiles, BESS characteristics, and economic parameters, is described in detail to ensure reproducibility of the results.

4.1. Network Topology and Parameters

The test system is based on the standard 33-bus radial distribution network adapted from [8] for BESS operation in distribution networks, which has been widely used to validate distribution system analysis and optimization methods. The network operates at a nominal voltage of 12.66 kV and a base power of 1,000 kVA. The system comprises 33 buses and 32 distribution lines, with a single substation located at bus 1 that serves as the slack bus. The general single-line diagram of the 33-bus grid is depicted in Figure 1.

The line parameters, including resistance R [Ω], reactance X [Ω], and thermal current limits $I_{\max}$ [A], are summarized in Table 2. These parameters are expressed in physical units (Ohms and Amperes) and represent a realistic medium-voltage distribution feeder. The load data, expressed in kW and kvar, are also provided for each bus, representing the peak demand at each location. The total active and reactive power demand of the system at peak conditions is approximately 3,715 kW and 2,300 kvar, respectively.

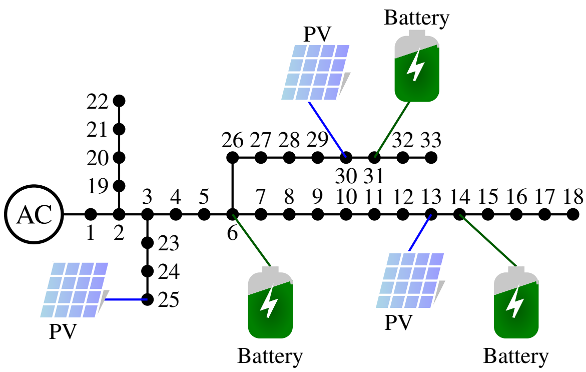

Figure 1. Single-line diagram of the modified 33-bus active distribution network.

Table 2. Line parameters and load data for the 33-bus distribution network.

From Bus	To Bus	R [Ω]	X [Ω]	P [kW]	Q [kvar]	$I_{\max}$ [A]
1	2	0.0922	0.0477	100	60	385
2	3	0.4930	0.2511	90	40	355
3	4	0.3660	0.1864	120	80	240
4	5	0.3811	0.1941	60	30	240
5	6	0.8190	0.7070	60	20	240
6	7	0.1872	0.6188	200	100	110
7	8	1.7114	1.2351	200	100	85
8	9	1.0300	0.7400	60	20	70
9	10	1.0400	0.7400	60	20	70
10	11	0.1966	0.0650	45	30	55
11	12	0.3744	0.1238	60	35	55
12	13	1.4680	1.1550	60	35	55
13	14	0.5416	0.7129	120	80	40
14	15	0.5910	0.5260	60	10	25
15	16	0.7463	0.5450	60	20	20
16	17	1.2890	1.7210	60	20	20
17	18	0.7320	0.5740	90	40	20
2	19	0.1640	0.1565	90	40	40
19	20	1.5042	1.3554	90	40	25
20	21	0.4095	0.4784	90	40	20
21	22	0.7089	0.9373	90	40	20
3	23	0.4512	0.3083	90	50	85
23	24	0.8980	0.7091	420	200	85
24	25	0.8960	0.7011	420	200	40
6	26	0.2030	0.1034	60	25	125
26	27	0.2842	0.1447	60	25	110
27	28	1.0590	0.9337	60	20	110
28	29	0.8042	0.7006	120	70	110
29	30	0.5075	0.2585	200	600	95
30	31	0.9744	0.9630	150	70	55
31	32	0.3105	0.3619	210	100	30
32	33	0.3410	0.5302	60	40	20

4.2. Load Profiles

The time-varying nature of the load demand is captured through normalized daily profiles that represent the typical consumption patterns of a distribution feeder. The active and reactive power demands at each bus are scaled by a common time-dependent factor derived from real load measurements. These profiles reflect the characteristic daily variations in electricity consumption, with peak demands typically occurring during morning and evening hours, and lower consumption during nighttime periods.

The active power demand factor $f_{P,t}$ and reactive power demand factor $f_{Q,t}$ at each time interval t are given by the first two columns of the matrix PVD in the implementation code. These factors represent the fraction of the peak load that is present at each hour of the day, with values ranging from approximately 0.6150 to 0.9560 for active power and from 0.5948 to 0.9797 for reactive power. The combined effect of these profiles results in a total daily energy consumption that reflects realistic operating conditions for a distribution network.

4.3. Photovoltaic Generation System

The test system incorporates three PV generation units installed at buses 13, 25, and 30. These units have rated capacities of 2,250 kW, 2,640 kW, and 1998 kW, respectively. These PV generators can be dispatched as a function of the grid requirements with the possibility of active and reactive power control.

The normalized irradiance profile $\rho_{i,t}$ for each PV unit is provided in the third column of the PVD matrix. This profile represents the fraction of the rated power that is available from the solar resource at each hour of the day. The typical daily pattern shows zero generation during nighttime hours (from 6:00 PM to 6:00 AM), with increasing generation during the morning hours, reaching a peak around noon, and declining in the afternoon. The maximum irradiance factor reaches approximately 0.626 p.u. at hour 12, reflecting the combined effects of solar position, cloud cover, and other atmospheric conditions.

The apparent power rating of each PV inverter is set equal to the rated active power of the PV generator, as is common practice in grid-connected PV systems where the inverter is sized to match the DC capacity. This assumption ensures that the inverter can handle the maximum power output of the PV array under standard test conditions.

4.4. Battery Energy Storage Systems

Three battery energy storage systems are installed at buses 6, 14, and 31, providing operational flexibility to the network. The BESS units have energy capacities of 0.5 MWh, 1.0 MWh, and 0.6667 MWh, respectively, and are assumed to use lithium-ion battery technology with appropriate charging and discharging characteristics.

The key parameters of each BESS unit are summarized in Table 3, including the energy capacity E_b [MWh], maximum charging power $P_b^{\text{ch,max}}$ [MW] (negative), maximum discharging power $P_b^{\text{dis,max}}$ [MW] (positive), state-of-charge limits, initial and final SoC, and charging/discharging efficiencies.

Table 3. Technical parameters of the battery energy storage systems.

BESS	**Location**	E_b **[MWh]**	$P_b^{\text{ch,max}}$ **[MW]**	$P_b^{\text{dis,max}}$ **[MW]**	**SoC**$^{\min}$	**SoC**$^{\max}$	η_b^{ch}	η_b^{dis}
1	6	0.5000	-0.400	0.400	0.10	0.90	0.95	0.90
2	14	1.0000	-0.250	0.250	0.10	0.90	0.95	0.90
3	31	0.6667	-0.375	0.375	0.10	0.90	0.95	0.90

All BESS units are assumed to have an initial state-of-charge of 0.50 p.u. and a final state-of-charge of 0.50 p.u., ensuring cyclic operation over the 24-hour horizon. The charging and discharging efficiencies are set to 0.95 and 0.90, respectively, which are representative of modern lithium-ion battery systems. The self-discharge rate is assumed to be 0.2% per hour ($\sigma = 0.002$ p.u./h), a typical value for lithium-ion chemistry.

The apparent power rating of each BESS inverter is set to the maximum of the charging and discharging power ratings, reflecting the converter's capability to handle bidirectional power flow. This results in inverter ratings of 400 kVA, 250 kVA, and 375 kVA for BESS units 1, 2, and 3, respectively.

4.5. Daily Profiles and Economic Parameters

The complete set of daily profiles used in the study is presented in Table 4, which includes the normalized demand factors for active and reactive power, the PV generation availability factor, and the time-varying energy price. These profiles are synchronized with a 24-hour horizon with hourly resolution.

Table 4. Daily profiles for demand, PV generation, and energy price.

Hour	$f_{P,t}$	$f_{Q,t}$	$\rho_{i,t}$	λ_t **[p.u.]**	**Hour**	$f_{P,t}$	$f_{Q,t}$	$\rho_{i,t}$	λ_t **[p.u.]**
1	0.6551	0.6285	0.0000	0.8011	13	0.9439	0.9573	0.6181	0.9549
2	0.6302	0.6089	0.0000	0.7480	14	0.9313	0.9273	0.5572	0.9469
3	0.6156	0.6181	0.0000	0.7347	15	0.9254	0.8986	0.4524	0.9523
4	0.6158	0.5948	0.0000	0.7480	16	0.9226	0.9655	0.3205	0.9549
5	0.6446	0.6218	0.0000	0.7851	17	0.9081	0.9506	0.1769	0.9947
6	0.6989	0.7294	0.0000	0.8674	18	0.8886	0.8934	0.0507	1.0000
7	0.7342	0.7469	0.0454	0.9337	19	0.9462	0.9099	0.0005	0.9735
8	0.7935	0.8052	0.1842	0.9576	20	0.9562	0.9168	0.0000	0.9576
9	0.8433	0.8018	0.3410	0.9416	21	0.9155	0.9531	0.0000	0.9151
10	0.8762	0.8620	0.4816	0.9655	22	0.8478	0.8880	0.0000	0.8621
11	0.9170	0.8790	0.5737	0.9655	23	0.7683	0.7786	0.0000	0.7772
12	0.9460	0.9797	0.6257	0.9629	24	0.7030	0.7335	0.0000	0.7135

The energy price profile λ_t is expressed in per-unit values relative to a base price of 0.2705 USD/kWh. This profile represents the time-of-use tariff structure common in many distribution systems, with higher prices during peak demand periods (typically late afternoon and early evening) and lower prices during off-peak hours (nighttime and early morning). The price factor ranges from approximately 0.714 p.u. at hour 24 to 1.000 p.u. at hour 18, reflecting the typical daily variation in wholesale electricity markets.

The economic parameters used in the objective function include a power loss factor $\beta^{\text{loss}} = 3\%$ to account for network losses, a reactive power penalty factor $\beta^{\text{Q}} = 20\%$ to capture the additional cost of reactive power flow, a PV O&M cost of 0.025 USD/kWh, a BESS O&M cost of 0.0225 USD/kWh, and a degradation cost coefficient of 10 USD per equivalent full cycle.

5. Computational Analysis

This section presents the computational results obtained from applying the proposed optimization framework to the modified 33-bus distribution network described in Section 4. The analysis is organized around seven distinct scenarios that progressively introduce distributed energy resources and reactive power control capabilities, allowing a comprehensive evaluation of their individual and combined impacts on the system's operational performance and energy procurement costs. The scenarios are designed to isolate the effects of different technologies and control strategies, providing valuable insights for distribution system operators and planners. Each scenario is simulated over a 24-hour horizon with hourly resolution, and the results are compared in terms of total daily operating cost and energy purchased from the substation. Since the model employs an aggregated single-node representation, voltage profiles are not computed; however, the reduction in reactive power procurement is indicative of improved network efficiency and reduced losses, which in practice would translate to better voltage profiles.

5.1. Scenario Definition

The seven scenarios considered in this study are defined as follows:

1. **Scenario 1 – Base Case:** The network operates without any distributed generation or energy storage systems. All load demands are supplied exclusively by the substation. This scenario serves as the reference for evaluating the benefits of integrating DERs.

2. **Scenario 2 – PV Generation Only:** The network incorporates the three photovoltaic generation units, which provide active power injection based on grid requirements. The PV units inject active power into the grid but do not provide reactive power support, meaning their reactive power output is fixed at zero. This scenario evaluates the impact of active power injection from renewable generation on operational costs under conditions where PV generation may be curtailed to maintain system balance. The reactive power capability of the PV inverters is intentionally deactivated to isolate the effects of active power displacement from the benefits of reactive power support.
3. **Scenario 3 – PV with Reactive Power Control:** The PV units are allowed to provide reactive power support within their inverter apparent power limits. The active power output remains determined by grid requirements, while the reactive power capability is fully utilized to reduce reactive power procurement from the substation. This scenario evaluates the additional economic benefits of reactive power compensation from PV inverters, which in practice would also contribute to voltage support and loss reduction.
4. **Scenario 4 – BESS Only (Active Power Only):** The network incorporates three BESS units that provide only active power services (charging/discharging) without reactive power capability. The batteries are scheduled to perform energy arbitrage and peak shaving while respecting their operational constraints. This scenario evaluates the impact of energy storage on operational costs.
5. **Scenario 5 – BESS with Reactive Power Control:** The BESS units provide both active and reactive power services within their inverter apparent power limits. This scenario evaluates the combined benefits of energy arbitrage and reactive power support from battery systems.
6. **Scenario 6 – PV Generation and BESS (Active Power Only):** Both PV units and BESS units are integrated into the network, but only active power services are provided. PV generation is dispatched according to grid requirements, and BESS provides only charging/discharging capabilities. This scenario evaluates the combined benefits of renewable generation and energy storage without reactive power coordination.
7. **Scenario 7 – Full Integration with Coordinated Active-Reactive Control:** All available resources (PV and BESS) are fully utilized with coordinated active and reactive power dispatch. PV generation is dispatched according to grid requirements while also providing reactive power support, and BESS units provide both active and reactive power services within their inverter capabilities. This scenario represents the complete proposed framework and demonstrates the maximum potential benefits of coordinated DER integration.

5.2. Scenario Results and Comparison

Table 5 summarizes the key performance indicators for all seven scenarios, including the total daily operating cost, energy purchased from the substation, active power losses, minimum voltage magnitude, and number of voltage violations. The results demonstrate the progressive benefits of integrating distributed energy resources and enabling reactive power control.

Table 5. Performance indicators for the seven scenarios.

Scenario	Energy Cost [USD/day]	PV Cost [USD/day]	BESS Cost [USD/day]	Degradation Cost [USD/day]	Total Cost [USD/day]	Reduction [%]
1	22,787.63	0.00	0.00	0.00	22,787.63	0.00
2	15,320.98	699.19	0.00	0.00	16,020.18	29.70
3	10,899.92	699.19	0.00	0.00	11,599.11	49.10
4	22,798.29	0.00	1.20	0.65	22,800.15	-0.05
5	20,423.55	0.00	1.21	0.62	20,425.38	10.37
6	14,907.52	744.98	75.42	24.00	15,751.92	30.88
7	10,486.45	744.98	75.42	24.00	11,330.85	50.28

The base case scenario (Scenario 1) represents the conventional operation of the distribution network without any distributed energy resources, where all load demand is supplied exclusively by the substation, resulting in a total daily operating cost of 22,787.63 USD/day. This value serves as the benchmark for all subsequent scenarios. In Scenario 2, the integration of PV generation reduces the energy procurement cost from 22,787.63 USD/day to 15,320.98 USD/day, a substantial reduction of 7,466.65 USD/day, though the PV operation and maintenance cost amounts to 699.19 USD/day, resulting in a total daily cost of 16,020.18 USD/day, representing a 29.70% reduction compared to the base case. Since reactive power support is not provided, the substation must still supply all reactive power requirements, demonstrating that while renewable generation provides significant economic benefits through active power displacement, additional benefits can be unlocked through reactive power coordination.

In Scenario 3, the reactive power capability of the PV inverters is enabled, allowing them to reduce reactive power procurement from the substation. The energy procurement cost decreases dramatically to 10,899.92 USD/day, representing a reduction of 11,887.71 USD/day compared to the base case, while the PV O&M cost remains unchanged at 699.19 USD/day, resulting in a total cost of 11,599.11 USD/day, which corresponds to a 49.10% reduction. This substantial improvement demonstrates that reactive power control from PV inverters provides significant economic benefits beyond the simple displacement of active power, as the reduced reactive power procurement lowers the overall energy cost, reflecting the avoided penalties and losses associated with reactive power flow. Although the aggregated model does not compute voltage profiles, this reduction in reactive power procurement would, in a real network, contribute to improved voltage regulation and reduced feeder losses.

Scenario 4 considers the integration of BESS units operating with active power only, meaning that the batteries are scheduled solely for energy arbitrage and peak shaving without providing reactive power support. The results show a total daily cost of 22,800.15 USD/day, which represents a marginal increase of 0.05% with respect to the base case. This apparently counterintuitive result can be explained by the fact that, under the particular price profile considered in this study, the arbitrage revenue obtained from shifting energy from low-price to high-price periods is almost entirely offset by the combined effect of the battery degradation cost (0.65 USD/day) and the BESS operation and maintenance cost (1.20 USD/day). In other words, the equivalent full-cycle degradation cost and the O&M cost per MWh of throughput consume nearly all of the price spread captured by the battery, leaving a small net deficit relative to the base case. This finding underscores the importance of reactive power coordination, because, as shown in Scenario 5, when the BESS is also allowed to provide reactive power support, the additional revenue stream compensates for the cycling costs and restores the economic viability of the storage installation.

Scenario 5 enables reactive power control from the BESS inverters, yielding a significant improvement in performance with the energy procurement cost decreasing to 20,423.55 USD/day, representing a reduction of 2,364.08 USD/day compared to the base case, while the BESS O&M and degradation costs amount to 1.21 USD/day and 0.62 USD/day, respectively, resulting in a total cost of 20,425.38 USD/day, which corresponds to a 10.37% reduction. This result demonstrates that the ability of BESS units to provide reactive power support is critical for realizing their full economic potential, as the combination of energy arbitrage and voltage support creates significant value by reducing reactive power flows and associated losses, improving the overall efficiency of the network. Scenario 6 integrates both PV generation and BESS units, but only active power services are provided, with PV generation dispatched according to grid requirements and BESS providing only charging and discharging capabilities. The energy procurement cost is reduced to 14,907.52 USD/day, while the PV O&M cost amounts to 744.98 USD/day, and the BESS O&M and degradation costs total 75.42 USD/day and 24.00 USD/day, respectively, resulting in a total daily cost of 15,751.92 USD/day, representing a 30.88% reduction compared to the base case. This shows that combining renewable generation and energy storage yields significant economic advantages, although the performance is only marginally better than in Scenario 2. This suggests that, without reactive power support, adding BESS provides limited incremental value beyond what PV alone can achieve.

Finally, Scenario 7 represents the complete proposed framework featuring coordinated active and reactive power dispatch from both PV and BESS units, achieving the best overall performance with the energy procurement cost reduced to 10,486.45 USD/day, while the PV O&M cost amounts to 744.98 USD/day, and the BESS O&M and degradation costs total 75.42 USD/day and 24.00 USD/day, respectively. The total daily cost is 11,330.85 USD/day, representing a 50.28% reduction compared to the base case, which is the largest reduction among all scenarios. This substantial improvement demonstrates the synergistic benefits of coordinating active and reactive power from both PV and BESS units, where the PV units provide active power while also contributing to voltage support through reactive power control, and the BESS units perform energy arbitrage while also providing reactive power support. The degradation cost of 24.00 USD/day reflects the cycling of the batteries, which is carefully managed by the optimization to balance energy arbitrage benefits against battery wear. The computational analysis reveals several important findings: PV integration alone reduces total costs by 29.70%, while enabling reactive power control from PV inverters provides an additional 19.40% cost reduction; BESS units operating with only active power services provide minimal economic benefits; enabling reactive power control from BESS units provides a 10.37% cost reduction; and the full integration of both PV and BESS with coordinated active-reactive control achieves the best performance with a 50.28% cost reduction. These findings confirm that the proposed optimization framework, which coordinates active and reactive power dispatch from PV and BESS units, provides significant economic and technical benefits for active distribution networks, enabling distribution system operators to fully utilize the capabilities of distributed energy resources while maintaining voltage security and power quality.

6. Conclusions and Future Work

This paper has presented a novel convex optimization framework for the optimal day-ahead scheduling of battery energy storage systems in active distribution networks, addressing critical research gaps in the coordinated dispatch of active and reactive power, degradation-aware operation, and computational tractability. The proposed framework formulates the problem as a mixed-integer nonlinear programming model that simultaneously optimizes the active and reactive power dispatch of BESS units while enforcing the power balance equation for an aggregated single-node representation of the distribution network. Unlike most existing approaches that treat active and reactive power independently, the proposed formulation exploits the inverter capabilities of modern BESS units, enabling them to provide both energy arbitrage and reactive power support services at the same time. A detailed battery degradation cost model is incorporated using an equivalent full-cycle counting approach based on the cumulative variation of the state-of-charge trajectory, capturing the economic impact of cycling on battery lifetime. The resulting MINLP is exactly reformulated as a mixed-integer second-order cone program through the convex reformulation of the apparent power constraints and the linearization of the absolute value terms in the degradation cost, preserving convexity and enabling efficient solution using state-of-the-art optimization solvers. The framework is implemented using MATLAB CVX with the Gurobi solver and validated on a modified 33-bus radial distribution network incorporating three PV generation units and three BESS units, with detailed time-varying load profiles, solar irradiance profiles, and energy price data representing realistic Colombian distribution system conditions.

The computational analysis, organized around seven distinct scenarios that progressively introduce distributed energy resources and reactive power control capabilities, demonstrates the significant economic benefits of the proposed framework. The numerical results show that the proposed framework achieves a total daily cost reduction of up to 50.28% compared to the base case without distributed resources, with PV integration alone reducing costs by 29.70%, and enabling reactive power control from PV inverters providing an additional 19.40% cost reduction. Furthermore, while BESS units operating with active power-only services provide minimal economic benefits, enabling reactive power control from BESS units yields a 10.37% cost reduction, and the full integration of both PV and BESS with coordinated active-reactive control achieves the best performance with a 50.28% cost reduction. These findings confirm that coordinated active-reactive power dispatch, combined with degradation-aware scheduling, provides substantial economic benefits for distribution systems with integrated renewable sources and energy storage. The results also highlight the critical importance of reactive power capabilities in realizing the full economic potential of BESS units, as active power-only operation provides negligible benefits under the considered price profiles and network configurations. Although the aggregated model does not compute voltages or branch flows, the substantial reduction in reactive power procurement indicates that, in practice, these strategies would also contribute to improved voltage regulation and reduced losses.

Several directions for future research remain open to extend and enhance the proposed framework. First, the current formulation employs an aggregated single-node representation of the distribution network, which does not capture detailed voltage profiles or branch power flows. Future work will extend the framework to a multi-node formulation with full AC power flow constraints, enabling a more comprehensive analysis of voltage support and network security. Second, while the degradation model captures cycling effects through an equivalent full-cycle counting approach, more sophisticated degradation models could be incorporated, including temperature-dependent aging, depth-of-discharge effects, and calendar aging, to provide a more accurate representation of battery lifetime. Third, a natural and important extension of this work is the incorporation of uncertainty management techniques to account for forecast errors in load demand, photovoltaic generation, and energy prices. In particular, the deterministic exact MISOCP proposed here could be extended toward a two-stage stochastic programming framework, in which first-stage BESS scheduling decisions are made before the uncertainty is realized and second-stage recourse actions are taken afterward. This would allow the system operator to hedge against adverse realizations while still exploiting the computational tractability of the convex reformulation. Alternatively, robust optimization or distributionally robust optimization could be employed to provide guarantees on worst-case performance without requiring full knowledge of the probability distributions of the uncertain parameters. Such extensions would significantly broaden the practical applicability of the proposed approach to real-time operation under uncertainty. Fourth, the methodology could be extended to include other distributed energy resources, such as wind turbines, diesel generators, and electric vehicle charging stations, enabling a more comprehensive framework for DER coordination. Finally, the application of the proposed framework to real-world distribution feeders, with validation against actual operational data, would provide valuable insights into its practical applicability and potential for commercial deployment. The source code of the proposed methodology is made publicly available to encourage further research and adoption by the scientific community.

ACKNOWLEDGEMENTS

The authors acknowledge the support provided by Thematic Network 723RT0150 “Red para la integración a gran escala de energías renovables en sistemas eléctricos (RIBIERSE-CYTED)” funded by the 2022 Call for Thematic Networks by the Ibero-American Program of Science and Technology for Development (CYTED in Spanish).

Declaration of AI Use

The authors acknowledge the assistance of the DeepSeek AI language model in refining the manuscript’s language and structure. The tool was used solely for editorial purposes—such as rephrasing, grammar correction, and improving readability—whereas all technical formulations, methodological developments, numerical simulations, and scientific interpretations were conceived and executed by the authors.

REFERENCES

[1] Herman Zahid, Adil Zulfiqar, Muhammad Adnan, Muhammad Sajid Iqbal, Anwar Shah, and Salah Eldeen Gasim Mohamed. Global renewable energy transition: A multidisciplinary analysis of emerging computing technologies, socio-economic impacts, and policy imperatives. *Results in Engineering*, 26:105258, 2025. ISSN 2590-1230. 10.1016/j.rineng.2025.105258.

[2] Ganiyu Bolawale Omotoye, Binaebi Gloria Bello, Sunday Tubokirifuruar Tula, Azeez Jason Kess-Momoh, Andrew Ifesinachi Daraojimba, and Adedayo Adefemi. Navigating global energy markets: A review of economic and policy impacts. *International Journal of Science and Research Archive*, 11(1):195–203, January 2024. ISSN 2582-8185. 10.30574/ijsra.2024.11.1.0029.

[3] Fatma Avli Firis and Ali Rifat Boynuegri. Cycle-aware optimization of battery storage in distribution networks under load and market uncertainty. *Journal of Energy Storage*, 138:118668, December 2025. ISSN 2352-152X. 10.1016/j.est.2025.118668.

[4] Varathan G. and Belwin Edward J. A review of uncertainty management approaches for active distribution system planning. *Renewable and Sustainable Energy Reviews*, 205:114808, November 2024. ISSN 1364-0321. 10.1016/j.rser.2024.114808.

[5] N. Hatziargyriou, G. Joos, and C. Schwaegerl. *Operation of Battery Energy Storage Systems in Distribution Networks*, pages 1–55. Springer Nature Switzerland, 2025. ISBN 9783030876937. 10.1007/978-3-030-87693-7_27-1.

[6] Oscar Danilo Montoya and Walter Gil-González. Dynamic active and reactive power compensation in distribution networks with batteries: A day-ahead economic dispatch approach. *Computers & Electrical Engineering*, 85:106710, 2020. ISSN 0045-7906. 10.1016/j.compeleceng.2020.106710.

[7] Víctor Manuel Garrido-Arévalo, Walter Gil-González, Oscar Danilo Montoya, Luis Fernando Grisales-Noreña, and Jesús C. Hernández. Optimal Dispatch of DERs and Battery-Based ESS in Distribution Grids While Considering Reactive Power Capabilities and Uncertainties: A Second-Order Cone Programming Formulation. *IEEE Access*, 12:48497–48510, 2024. ISSN 2169-3536. 10.1109/access.2024.3382940.

[8] Luis Fernando Grisales-Noreña, Daniel Sanin-Villa, and Oscar Danilo Montoya. Parallel Metaheuristic-Based Optimization for Electric Vehicle Charging Station Integration and Sizing in Distribution Systems. In *IOCEN 2026*, IOCEN 2026, page 7. MDPI, 2026. 10.3390/engproc2026147007.

[9] Víctor M. Garrido-Arévalo, Oscar Danilo Montoya, Walter Gil-González, Luis Fernando Grisales-Noreña, and Jesus C. Hernández. An SDP relaxation in the complex domain for the efficient coordination of BESS and DGs in single-phase distribution grids while considering reactive power capabilities. *Journal of Energy Storage*, 90:111913, 2024. ISSN 2352-152X. 10.1016/j.est.2024.111913.

[10] Diego Jose da Silva, Edmarcio Antonio Belati, Jesús M. López-Lezama, and Mahdi Pourakbari-Kasmaei. Optimal Allocation and Operation of Battery Energy Storage Systems With Photovoltaic Generation in Modern Distribution Networks: A New Hybrid Approach. *IET Renewable Power Generation*, 19(1), January 2025. ISSN 1752-1424. 10.1049/rpg2.70114.

[11] Andrea Isella and Davide Manca. A framework for the design of battery energy storage systems in Power-to-X processes. *Journal of Energy Storage*, 123:116744, 2025. ISSN 2352-152X. 10.1016/j.est.2025.116744.

[12] Luis Fernando Grisales-Noreña, Brandon Cortés-Caicedo, Oscar Danilo Montoya, Rubén Iván Bolaños, and César Augusto Marín Moreno. Nonlinear programming for BESS operation for the improvement of economic, technical and environmental indices by considering grid-connected and stand-alone networks: An application to the territory of Colombia. *Journal of Energy Storage*, 98: 112856, 2024. ISSN 2352-152X. 10.1016/j.est.2024.112856.

[13] Jiazhi Lei and Zhao Liu. Optimal allocation of ESSs in distribution networks considering uncertainties of battery capacity fading and operation strategies correlation. *International Journal of Electrical Power & Energy Systems*, 167:110548, 2025. ISSN 0142-0615. 10.1016/j.ijepes.2025.110548.

[14] Wencong Su, Jianhui Wang, Kuilin Zhang, and Alex Q. Huang. Model predictive control-based power dispatch for distribution system considering plug-in electric vehicle uncertainty. *Electric Power Systems Research*, 106:29–35, January 2014. ISSN 0378-7796. 10.1016/j.epsr.2013.08.001.

[15] Talha Rehman, Muhammad Ahsan Khan, Woon-Gyu Lee, and Hak-Man Kim. Resilience oriented coordinated optimal operation of distribution system with virtual power plant. *Sustainable Energy, Grids and Networks*, 46:102206, 2026. ISSN 2352-4677. 10.1016/j.segan.2026.102206.

[16] Mohamed Bahloul, Mohamed Daoud, and Shafi K. Khadem. Optimal dispatch of battery energy storage for multi-service provision in a collocated PV power plant considering battery ageing. *Energy*, 293:130744, April 2024. ISSN 0360-5442. 10.1016/j.energy.2024.130744.

[17] Chase Humiston, Mehmet Cetin, and Anderson Rodrigo de Queiroz. Evaluating battery degradation models in rolling-horizon bess arbitrage optimization. *Energies*, 19(4):1056, February 2026. ISSN 1996-1073. 10.3390/en19041056.

[18] Héctor Pinto Vega, Luis Fernando Grisales-Noreña, Fiderman Machuca-Martínez, Oscar Danilo Montoya, and Daniel Sanin-Villa. Cost-oriented scheduling of battery energy storage with wind turbines in distribution microgrids. *Journal of Energy Storage*, 167: 122470, 2026. ISSN 2352-152X. 10.1016/j.est.2026.122470.

[19] Alireza Soroudi. *Power System Optimization Modeling in GAMS*. Springer International Publishing, 2017. ISBN 9783319623504. 10.1007/978-3-319-62350-4.

[20] César Augusto Marín Moreno, Kevin Alexander Leyton-Valencia, Luis Fernando Grisales-Noreña, Rubén Iván Bolaños, and Jesús C. Hernández. Electric Vehicle Charging Stations in Colombian Active Distribution Networks: Models, Impacts, and Research Challenges. *Sci*, 8(5):119, May 2026. ISSN 2413-4155. 10.3390/sci8050119.

[21] Vanio F. S. Júnior, Renato S. F. Ferraz, Rafael S. F. Ferraz, Augusto C. Rueda-Medina, and Eduardo S. Palmeira. Allocation and Sizing of Distributed Energy Resources and Capacitor Banks Considering Network Reconfiguration Through Multi-Objective Optimization Algorithms. *IEEE Access*, 14:70941–70954, 2026. ISSN 2169-3536. 10.1109/access.2026.3681788.

[22] Jerzy Andruszkiewicz, Józef Lorenc, and Agnieszka Weychan. Determination of the Optimal Level of Reactive Power Compensation That Minimizes the Costs of Losses in Distribution Networks. *Energies*, 17(1):150, December 2023. ISSN 1996-1073. 10.3390/en17010150.

[23] Karim L. Anaya and Michael G. Pollitt. A social cost benefit analysis for the procurement of reactive power: The case of Power Potential. *Applied Energy*, 312:118512, April 2022. ISSN 0306-2619. 10.1016/j.apenergy.2022.118512.

[24] Hind Abdulla, Andrei Sleptchenko, and Ammar Nayfeh. Photovoltaic systems operation and maintenance: A review and future directions. *Renewable and Sustainable Energy Reviews*, 195:114342, May 2024. ISSN 1364-0321. 10.1016/j.rser.2024.114342.

[25] Fredy A. Sepulveda-Velez, Diego L. Talavera, Leonardo Micheli, and Gustavo Nofuentes. A Novel Approach to Assessing the Cost Competitiveness of Self-Consumption Photovoltaic Systems. *Applied Sciences*, 16(5):2425, March 2026. ISSN 2076-3417. 10.3390/app16052425.

[26] Masoume Shabani and Jinyue Yan. Optimization and evaluation of operational and economic performance of grid-connected battery storage at different stages of battery health. *Energy Conversion and Management: X*, 27:101113, 2025. ISSN 2590-1745. 10.1016/j.ecmx.2025.101113.

[27] Nan Chen, Junheng Gao, Lihui Gao, Shuanghao Yang, and Shouyan Chen. Economic dispatch of integrated energy systems taking into account the participation of flexible loads and concentrated solar power plants. *Energy*, 320:135222, April 2025. ISSN 0360-5442. 10.1016/j.energy.2025.135222.

[28] Chris Coey, Miles Lubin, and Juan Pablo Vielma. Outer approximation with conic certificates for mixed-integer convex problems. *Mathematical Programming Computation*, 12(2):249–293, February 2020. ISSN 1867-2957. 10.1007/s12532-020-00178-3.

[29] Gurobi Optimization, LLC. Gurobi Optimizer Reference Manual, 2026. URL `https://www.gurobi.com/documentation/11.0/refman/index.html`. Accessed: July 7th, 2026.

[30] Dayan Adionel Guimaraes, Giovanni Henrique Faria Floriano, and Lucas Silvestre Chaves. A Tutorial on the CVX System for Modeling and Solving Convex Optimization Problems. *IEEE Latin America Transactions*, 13(5):1228–1257, May 2015. ISSN 1548-0992. 10.1109/tla.2015.7111976.